CHAPTER 9. U-Pb DATING AND Hf ISOTOPIC COMPOSITION OF ZIRCON BY LASER ABLATION-MC-ICP-MS

Nuno Machado[1,2] and Antonio Simonetti[1]
1 - Centre de recherche en Géochimie isotopique et en Géochronologie - GEOTOP
2 - Département des Sciences de la Terre et de l'Atmosphère
Université du Québec à Montréal, CP 8888, Succ. Centre-Ville
Montréal, QC H3C 3P8; machado.nuno@uqam.ca

INTRODUCTION

In the last four decades, the U-Pb method of dating rocks has undergone several major revolutions. The early work of Silver & Deutsch (1963) reported the analysis of 200-300 milligrams of zircon, corresponding to $>10^4$ grains; the finds that air abrasion reduced or eliminated discordancy and that zircon could be hydrothermally dissolved together with the miniaturization of chemical procedures attaining Pb blanks in the picogram range (Krogh 1973, 1982a, b) highlight these radical changes. The construction of a high resolution ion microprobe to date zircon (Compston *et al*. 1984) heralded a new epoch in U-Pb dating by demonstrating that a single zircon crystal may record many more geological events than the rock containing it and that some zircon crystals are the oldest recognised terrestrial material.

In spite of the exciting opportunities created by these developments for dating a variety of geological processes, U-Pb geochronology does not lend itself to isotopic tracing of these processes. The advent of laser ablation-inductively coupled plasma mass spectrometry (LA-ICPMS) promises to be the next revolutionary step as it permits dating and acquiring isotopic data on the same mineral without extensive, additional sample preparation (i.e. ion exchange chromatographic separation for Pb, U and Hf required for TIMS analyses). Zircon is a case in point as it yields U-Pb ages and Hf isotopic characteristics.

Arguably, the LA-ICPMS method is in a state of flux due to its novelty in U-Pb dating and application to radiogenic isotope studies. In this chapter, we describe the main problems encountered in zircon dating, the evolving strategies to solve them and some promising applications. As we envision that a major contribution of the method will be Hf isotopic characterization of dated zircons, we present the methodology for Hf isotopic determinations and results obtained so far at UQAM's laboratory.

THE U-Pb SYSTEM

U-Pb geochronology is based on the natural decay of ^{238}U and ^{235}U to stable ^{206}Pb and ^{207}Pb with half lives of 4.468 and 0.704 billion years, respectively. Measurement of the U and Pb concentrations and Pb isotopic composition of a sample yields two independent ages: $^{206}Pb/^{238}U$ and $^{207}Pb/^{235}U$. Data are usually displayed in a $^{207}Pb/^{235}U$ vs. $^{206}Pb/^{238}U$ diagram (Fig. 9.1) where the points having the same $^{207}Pb/^{235}U$ and $^{206}Pb/^{238}U$ ages define the concordia line (Wetherill 1956). The $^{207}Pb/^{206}Pb$ age is represented in this diagram by the slope of the line defined by the origin and a point on concordia. Samples yielding the same $^{207}Pb/^{235}U$ and $^{206}Pb/^{238}U$ ages necessarily yield the same $^{207}Pb/^{206}Pb$ age and are deemed concordant. Such samples represent closed systems, that is, they have not lost or gained U or Pb since the time of crystallisation. Data can also be presented in a Tera-Wasserburg diagram (Tera & Wasserburg 1972) where $^{238}U/^{206}Pb$ is plotted against $^{207}Pb/^{206}Pb$ (Fig. 9.2), or in its equivalent $^{235}U/^{207}Pb$ vs. $^{206}Pb/^{207}Pb$ (Tatsumoto *et al*. 1972).

The mineral most commonly used to date rocks by the U-Pb system is zircon ($ZrSiO_4$) because it incorporates U in its structure where it replaces Zr, but accepts very little or no Pb at the time of crystallisation. Other minerals with possible high primary U/Pb (i.e. low common Pb content) used for U-Pb geochronology are monazite, titanite, allanite, xenotime, baddeleyite and perovskite.

Depending on its intrinsic characteristics and geological history, a mineral may yield discordant U-Pb ages. In general, it is possible to obtain a series of analyses defining a discordia line whose upper and lower intercept ages correspond to geologic events. Thus, in contrast to other dating methods, it is possible to obtain useful information even in the case where the

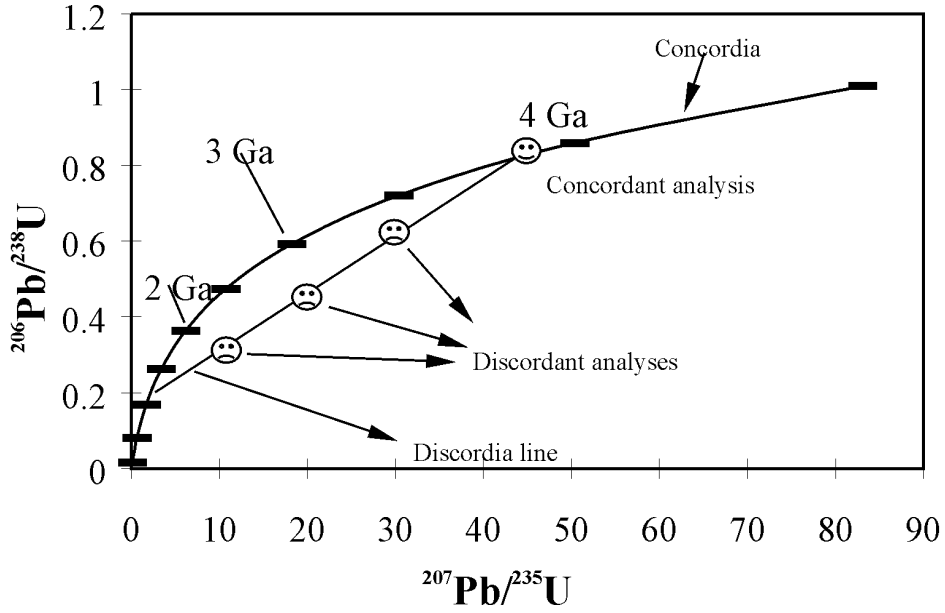

Figure 9.1 - Concordia diagram (Wetherill 1956).

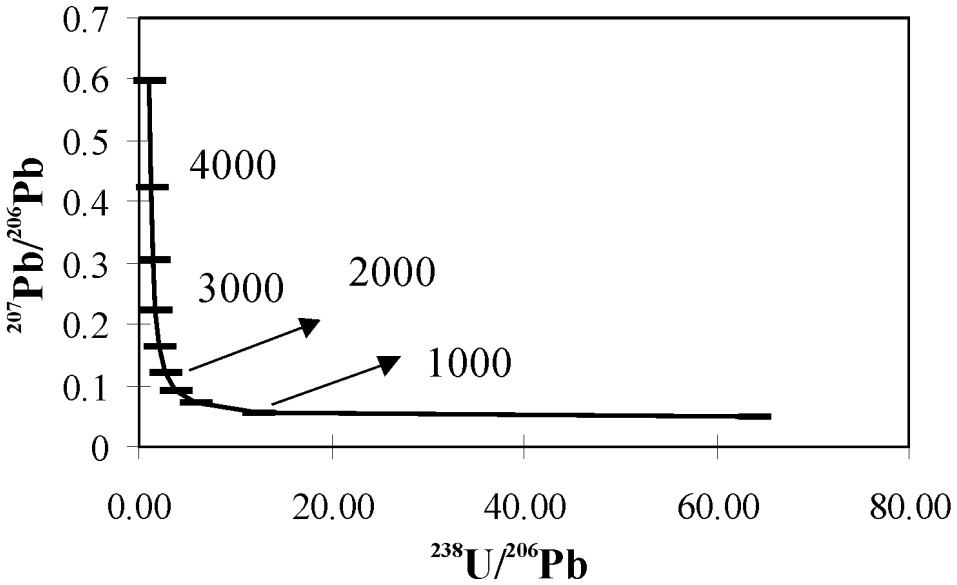

Figure 9.2 - Tera and Wasserburg (1972) concordia diagram.

selected samples represent open systems.

It is relevant to note that the uncertainty in measured ages (excluding the influence of analytical procedures) depends on the age of the sample, the Pb and U contents of the mineral, and on the internal precision of the measured isotopic ratios. For example, suppose that isotopic ratios are precise to 1% (standard error at 1σ) for a 1000 Ma old sample. This corresponds to uncertainties of ±9 Ma for the $^{206}Pb/^{238}U$ age, ±4 Ma for the $^{207}Pb/^{235}U$ age, and to ±20 Ma for the $^{207}Pb/^{206}Pb$ age. For a 3000 Ma sample, these values would be ±24, ±10 and ±16 Ma, respectively. This characteristic, intrinsic to the U-Pb system, has a

bearing on the evaluation of the performance of analytical methods.

The well established methods of U-Pb dating are conducted by isotope dilution-thermal ionisation mass spectrometry (ID-TIMS) and by ion probes, in particular by Sensitive High Resolution Ion Microprobe (SHRIMP). As a result of over thirty years of miniaturisation of chemical procedures and other methodological refinements (Krogh 1973, 1982a, b; Parrish 1987; Parrish and Krogh 1987) and the maturity of mass spectrometry technology, TIMS undoubtedly yields the most precise and accurate ages. However, it is laborious, destroys the sample and requires clean rooms and exacting maintenance procedures in order to yield reliable results. SHRIMP technology was developed specifically to date zircon and bypasses most of these disadvantages (Compston *et al*. 1984; Williams 1998); it offers the considerable advantage of *in situ* (Kröner *et al*. 2000) dating of different sectors in a single crystal and consumes a negligible amount of sample (see comparison in Stern 1997). However, this method is less precise and less adaptable for dating a variety of minerals compared to ID-TIMS (but see Stern & Berman 2000). Moreover, the equipment is rather expensive and requires special installation and maintenance.

U-Pb dating by laser ablation-ICPMS

This method involves the ejection of matter from a solid by a laser beam, ionisation of the ablated material by an argon plasma and the measurement of isotopic ratios by a mass spectrometer. The required equipment is a laser system and an inductively coupled plasma (ICP) instrument connected to a mass spectrometer (MS). For descriptions of these components the reader is referred to previous chapters.

The application of the laser ablation (LA) ICPMS technique to the determination of isotopic ratios led to the recognition that the measured ratios differ from the true values as determined by a variety of well established techniques (Figg & Kahr 1997, Longerich *et al*. 1996, Outridge *et al*. 1997). The analysis of elements with at least two natural stable isotopes (e.g. Sr, Hf) is simplified because their ratio can be used to normalise measured isotopic ratios of the same element. In the other cases, procedures have to be devised to determine or to compensate for isotopic and elemental fractionation. Dating minerals by the U-Pb method is a case in point because the only constant ratio is $^{238}U/^{235}U$, Pb having only one stable isotope, ^{204}Pb. In addition, as U and Pb are present in trace amounts in the minerals most amenable to dating and the amount of Pb depends on U content and age, analyte intensity constrains both the uncertainty of the measured ages and the youngest age that can be determined. Below, we consider the parameters affecting U-Pb age determinations.

Parameters controlling analyte intensity and U/Pb values

These can be considered in two categories, one pertaining to sample characteristics and the other related to analytical conditions. As mentioned above, the higher the U contents and the older the age of the mineral, the higher the potential Pb signal intensity. The size of the crystal or grain also influences the signal intensity because a larger grain can be analysed with a wider laser beam thus yielding higher signal intensity and more precise ratios than a narrower beam of the same fluence. Fig. 9.3 illustrates this effect. Alternatively, other laser ablation protocols used to obtain higher and more stable ion signal intensities (hence more precise U-Pb ages) include 'rastering' or 'line profiling' (Horstwood *et al*., 2000). For a homogeneous sample of a given age, the only characteristics impacting on the U/Pb value are inclusions and imperfections such as fractures. It has been shown that colourless inclusions strongly affect even $^{207}Pb/^{206}Pb$ values (Machado and Gauthier 1996) and they also cause instabilities in $^{206}Pb/^{238}U$ values. Fractures and incipient parting planes diffract the laser beam thus causing significant U/Pb variations. Therefore, selecting limpid crystals is as important to obtain the best results by LA-ICPMS as it is by ID-TIMS.

The analytical parameters affecting U-Pb results are considered next.

Laser type

Ideally, for geochemical analysis laser interaction with matter would be limited to the transfer of photon energy to the solid to break bonds and liberate atomic/molecular species. For complex materials, this would lead to stoichiometric ablation and the production of ≤1 μm particles to be subsequently efficiently

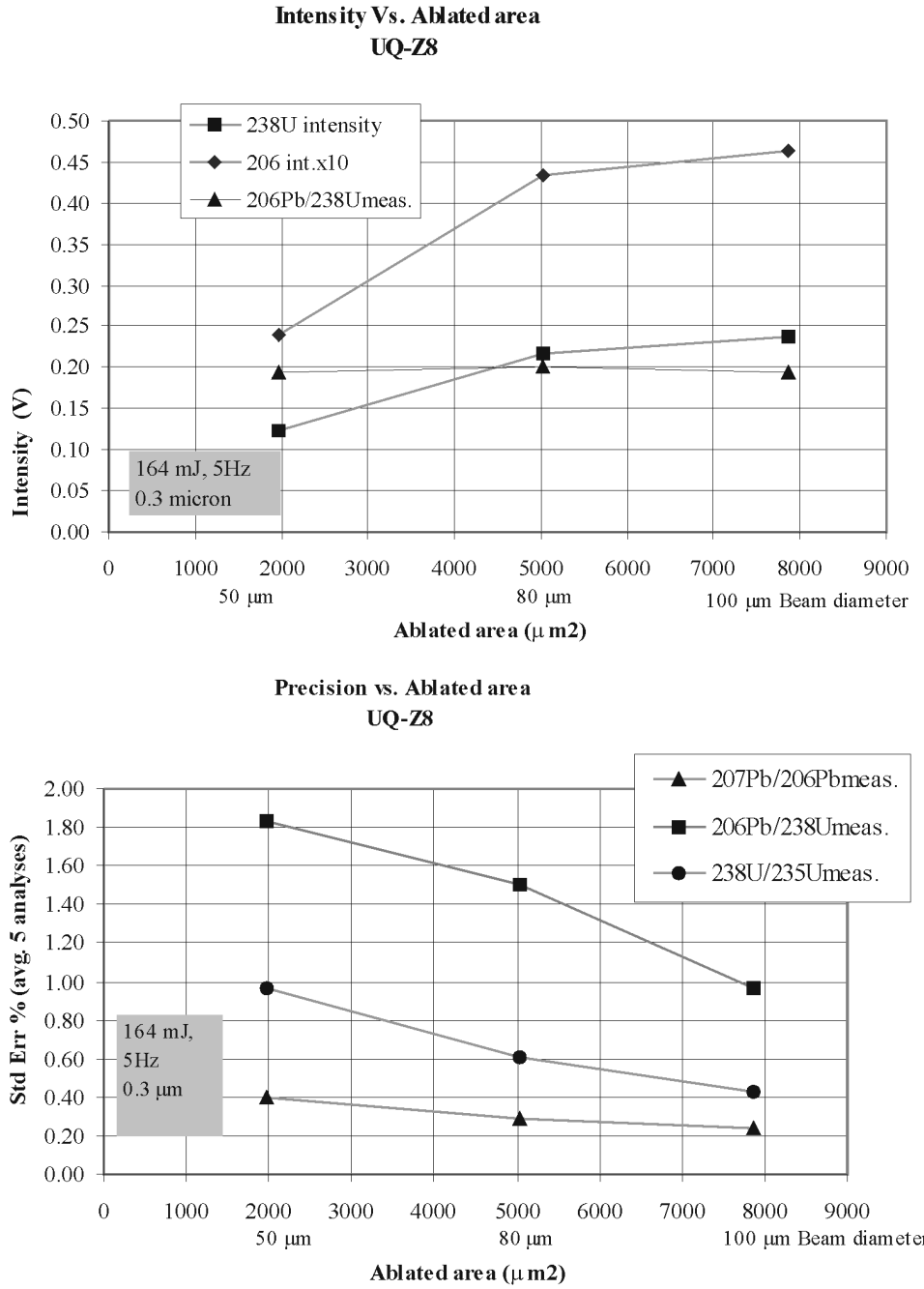

Figure 9.3 - Influence of laser beam diameter on signal intensity and precision of measured ratios.

ionized in the ICP plasma. However, laser-solid interaction involves a complex series of photophysical and photochemical effects, the relative importance of each depending, among other factors, on the laser wavelength, intensity and pulse duration and on the response of the irradiated material. For zircon, in common with inorganic ceramics and insulators, photophysical processes dominate. Compositional changes due to laser irradiation have not been reported for these materials, and Zr:Si values are identical for non-irradiated zircon and for ablated zircon

blanketing the surface around pit craters. Whether Hf and other trace elements also behave congruently is not known. Empirical evidence and analogy with similar materials suggest that laser-zircon interaction is probably dominated by thermal and bond-breaking effects.

The earlier attempts to date zircon using laser ablation employed Nd:YAG lasers operating at the 1064 nm fundamental wavelength with 2-6 mJ/pulse. Irradiating zircon with this infrared laser frequently causes cracking and ejection of molten $ZrSiO_4$ droplets up to ca. 20 μm. The plasma plume formed above the ablation pit is opaque to the IR radiation leading to strong heating of the plume and large thermal gradients. This may be the main source of elemental-isotopic fractionation observed when ablating zircon. The variability of the U/Pb isotopic ratios during a single analysis could exceed ±200% of the true values and precluded their use for geochronology. Better reproducibility was obtained for $^{207}Pb/^{206}Pb$ values which yielded ages precise to 0.5-6% for zircons with a minimum of ca. 30 ppm Pb (Fryer *et al*. 1993, Feng *et al*. 1993). In spite of these limitations, useful data could be obtained on detrital zircon and on metamorphic zircon and monazite (Machado and Gauthier 1996, Machado *et al*. 1996, Scott and Gauthier 1996).

The fact that elemental fractionation during ablation decreases at shorter wavelengths (Geertsen *et al*. 1994, Figg *et al*. 1998) prompted the use of frequency-quadrupled and quintupled Nd:YAG lasers emitting at 266 and 213 nm and of ArF Excimer lasers operating at 193 nm. Many inorganic materials have higher absorptivity at UV than at IR wavelengths and their interaction with UV radiation is dominated by thermal effects and the production of defect centres or radiative interactions with existing centres or trace components (Duley 1996). This leads to a more efficient coupling between laser and sample as expressed by the absence of fractures, cleaner pits and ejection of particles of smaller size. Hirata and Nesbitt (1995) showed that precisions of 0.6-5% and 3-20% for $^{207}Pb/^{206}Pb$ and $^{206}Pb/^{238}U$, respectively, could be attained. Applications of 266 nm radiation to the analyses of zircon can be found in Griffin *et al*. (2000) and Fernández-Suárez *et al*. (1999, 2000).

Comparisons of ablation characteristics between solid-state lasers emitting at 266 nm and ArF Excimer lasers (193 nm) indicate the latter yield more stable signals and lower or negligible elemental fractionation (Günther *et al*. 1997, Günther and Heinrich 1999). The reasons for these differences are still not well understood but the higher photon energy of excimer lasers may induce multiphoton sample decomposition with less significant photothermal effects. This results in overall smaller particle size, which can be more efficiently ionised at the ICP torch. However, given the variety of the mass spectrometers coupled to laser systems and the newness of the technology, at present it is unsound to compare the analytical performance of different instrumental configurations. Nevertheless, precisions of ≤2.0% for $^{206}Pb/^{238}U$ and $^{207}Pb/^{206}Pb$ and ≤3.0% for $^{207}Pb/^{235}U$ have been reported for Neoproterozoic and older zircons with U contents greater than ca. 65 ppm (Horn *et al*. 2000). These data where obtained with a 193 nm excimer laser coupled to a VG Elemental PQII+ quadrupole ICPMS. Combining sample ablation with solution nebulisation allowed a mass bias correction to be applied to the unknowns. Mass discrimination was also found to vary with spot size but not with repetition rate.

Here, we present U-Pb data obtained with a similar laser system coupled to a Micromass IsoProbe, a multicollector-magnetic sector mass spectrometer, which does not show statistically significant mass discrimination for $^{207}Pb/^{206}Pb$ and $^{206}Pb/^{238}U$ (Fig. 9.4) for spot sizes in the 50-100 μm range. A similar feature was also noted for laser ablation experiments using a VG Elemental P54 multicollector mass spectrometer coupled to a 266 nm UV laser (Parrish *et al*., 1999). These results indicate that although wavelength strongly controls mass fractionation, other factors must also contribute to it. One of these is the type of sample cell used.

Ablation cell

Several cell designs have been implemented for laser ablation but it is practically impossible to judge their relative efficiency because they are used with different laser and ICPMS systems. Design principles can be found in Fryer *et al*. (1995), and principles together with a comparison between different cells in Arrowsmith (1990).

The New Wave Research-Merchantek system at UQAM has a cell similar to that

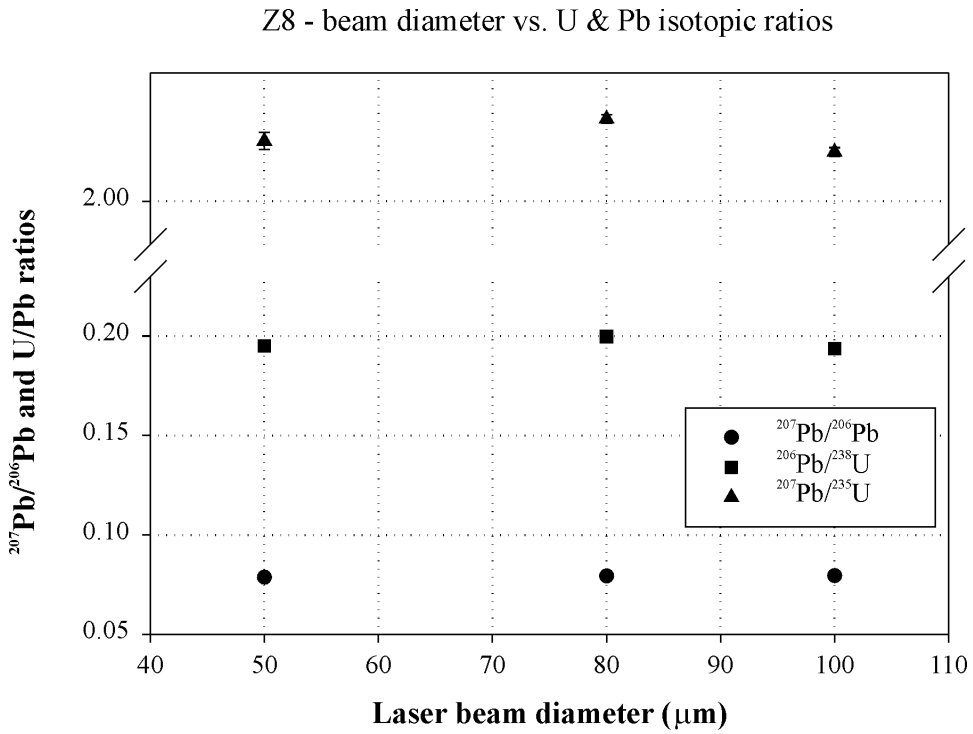

Figure 9.4 - Laser beam diameter vs. U and Pb isotopic ratios showing no significant variation in ratios with beam diameter. Symbols include error bars. Higher $^{207}Pb/^{235}U$ variability is due to lower signal intensity compared to intensities for ^{206}Pb and ^{238}U.

described by Fryer *et al*. (1995) and is provided with a needle to direct the entraining gas at the ablation spot. This design ("jet-cell"), a modification of the original by Sterling Shaw at Macquarie University and popularised by the MUN lab, is supposed to lower element fractionation. However, our experience with this cell design yields results contradictory with these earlier findings. Its use at different Ar flow rates not only caused variable, uncontrollable U/Pb fractionation but dramatically decreased signal intensity when compared to results obtained with the same cell but without the needle. In this case, the entrance hole is located at the base of the cell opposite to the exit orifice. Our results may indicate that among other factors, the efficiency of the jet-cell may depend on the size of the particles generated by the laser, which in turn are dependent on laser wavelength and energy.

Gaseous ablation medium

Ablation is usually performed in Ar, He, He+Ar, or N_2+Ar atmospheres that transports the suspended sample particles to the ICP. The gas flow rate can be adjusted in several ways, usually to yield the maximum signal intensity. However, this may not be the best adjustment because $^{206}Pb/^{238}U$ fractionation varies with gas flow. This effect has not been widely reported but may be significant in some instrumental configurations. We found significant variations in signal intensity and U/Pb values for a given set of analytical conditions (laser power, beam diameter, repetition rate, etc.) as shown in Figure 9.5: ^{206}Pb and ^{238}U signals vary with gas flow and the $^{206}Pb/^{238}U$ values increase from 0.186 at low flow rates to 0.317 at 0.48 l/min. The value for a concordant analysis is 0.194. At higher flow rates, the analytes' intensities oscillate rhythmically suggesting that the suspended particles are swirled around the ablation chamber and periodically pass over the exit hole where some of them are caught by suction. Therefore, the shape of the ablation chamber and the gas flow control the hydrodynamic regime undergone by the suspended particles.

The U/Pb fractionation may be related to the size of particles transported to the ICP torch.

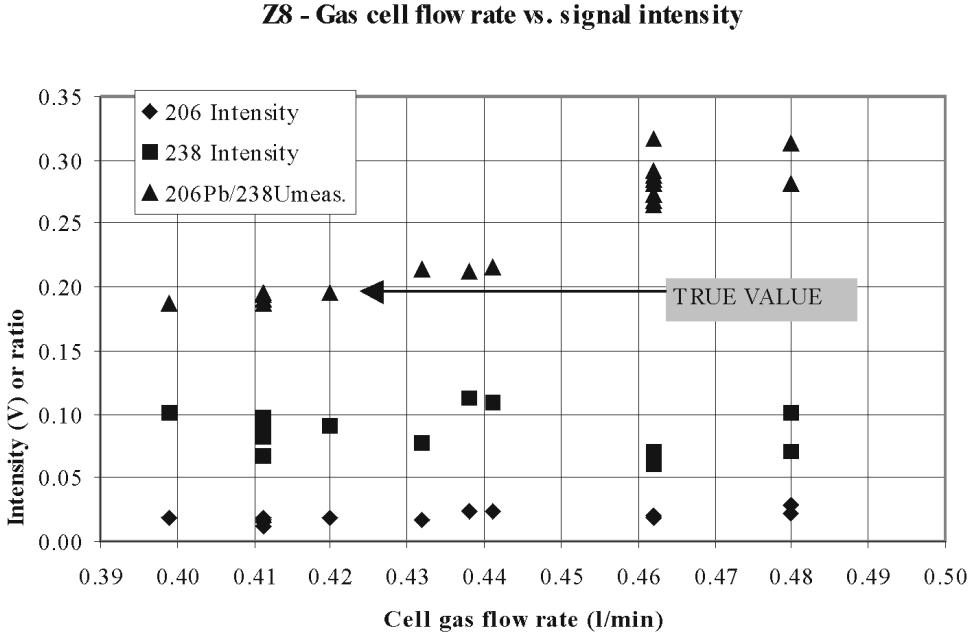

Figure 9.5 - Diagram showing variations in analyte intensity and in $^{206}Pb/^{238}U$ at several Ar flow rates in the sample cell.

Experiments carried out with an on-line particle counter reveal that smaller particles have a different composition from larger ones (Figg *et al*. 1998; Chenery *et al*. 1992). This seems to be confirmed in relation to laser power and wavelength at certain wavelengths - the longer wavelengths and higher power produce larger particles in the long UV range.

Performing ablation under He or an Ar/He mix yields not only less fractionated U/Pb ratios but also increases signal intensity (Eggins *et al*, 1998, Günther and Heinrich 1999). This is in agreement with studies of thin-film growing techniques by laser ablation-vapour deposition showing that different gases have diverse effects on the yield and grain size of the films (e.g. Rouleau *et al*. 1996 and references therein). It is speculated that lighter gas enhances diffusion of the plasma plume formed at the laser-sample interface thus decreasing thermal effects on the plume. The precise mechanism for the lesser fractionation and higher yield with He and He-Ar mixtures remains unclear. A systematic study on a single instrument of the influence of specific gases or gas mixtures on elemental/isotopic fractionation has not been published. However, we are presently conducting a comparative study between ablation in Ar vs. He atmospheres (Machado & Simonetti 2001).

Laser focus

Focusing the laser beam on the sample surface is achieved most commonly through a video camera coupled to a microscope. Usually, there is some way of ensuring that the visual focus corresponds to the best beam focus, that is, to the smallest beam diameter at the sample surface.

This parameter has to be carefully monitored because slight variations in the focus position cause variations in the U and Pb intensities and $^{206}Pb/^{238}U$ values. This is shown graphically in Figure 9.6 where this ratio varies between 0.180 and 0.214.

Surface roughness

Another poorly documented parameter is the influence of the sample surface roughness on the uncertainty of elemental and isotopic ratios. Our experiments on zircon UQ-Z8, an in-house standard, reveal an increase in precision for $^{206}Pb/^{238}U$ and a decrease for $^{207}Pb/^{235}U$ with roughness, from 0.3 μm to 9 μm (Fig. 9.7). The effect on the $^{207}Pb/^{206}Pb$ is minimal.

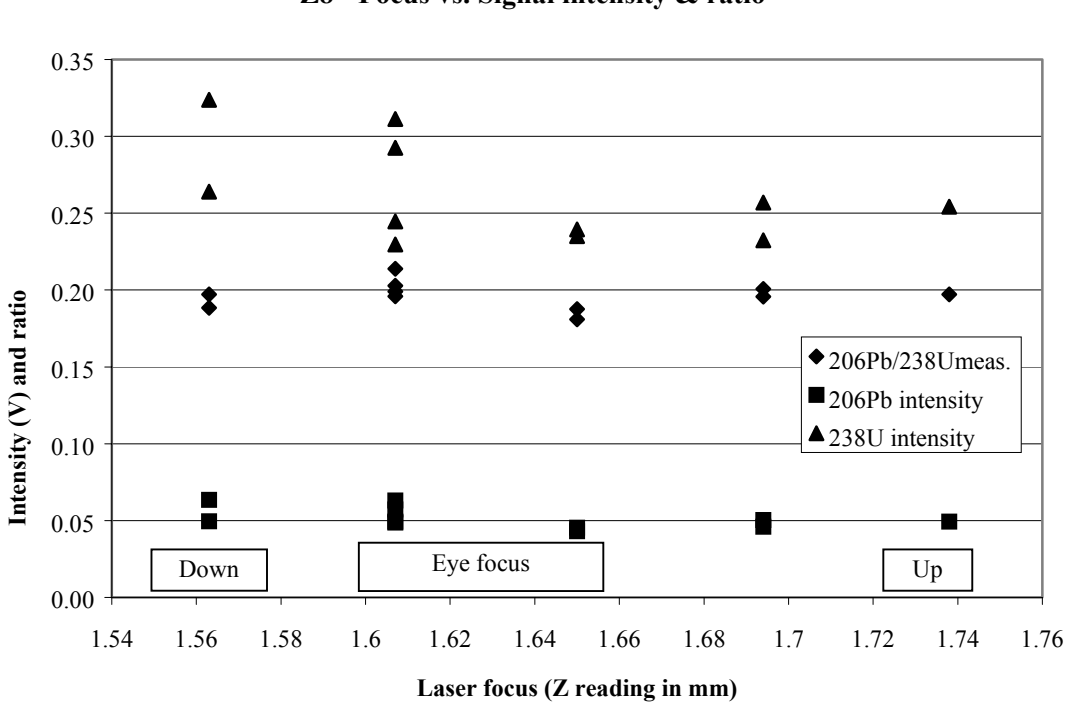

Figure 9.6 - Diagram showing the variability of ^{206}Pb and ^{238}U signal intensities and $^{206}Pb/^{238}U$ values as a function of laser focus position.

Analytical strategies

In order to obtain precise and accurate U-Pb ages, different analytical approaches have been followed. Regarding mass spectrometry, the current trend is the use of magnetic sector analyzers with wide flight tubes, allowing a mass spread of ca. 15% coupled to a bank of several collectors (multicollector ICPMS or MC-ICPMS). This permits the simultaneous measurement of all the Pb and U isotopes of interest (^{204}Pb to ^{238}U) and is better suited to the analysis of transient signals than single collector mass spectrometers.

To solve the problem of elemental-isotopic mass bias, both internal and external standardization methods have been proposed. In the former, a Tl solution is analyzed during ablation and the $^{203}Tl/^{205}Tl$ value used to correct Pb isotopic values. U/Pb ratios may be corrected for mass bias based on the $^{235}U/^{205}Tl$ value of a well calibrated solution aspirated into the ICP source (both methods used by Horn *et al*., 2000). Mass bias correction of measured Pb isotope ratios using a known Tl isotopic value assumes that the latter fractionation is identical to that of Pb, a feature which is not necessarily accurate (e.g. Thirlwall, 2000). Some instrumental configurations do not permit simultaneous analysis of ablated material and of a solution, thus the use of an external standard is required. A matrix-matched standard is preferable because different minerals have different absorptivities for each laser wavelength. This method is being used in our and other laboratories (e.g. Fernández-Suárez *et al*. 2000). However, it suffers from the disadvantage that it requires a variety of well dated minerals which are destroyed during analysis, and that there is no internationally recognized standard for U-Pb geochronology.

A comparison of these two methods is not viable at present. The sparse available data is mostly preliminary and produced in variable analytical conditions using different instrumental configurations.

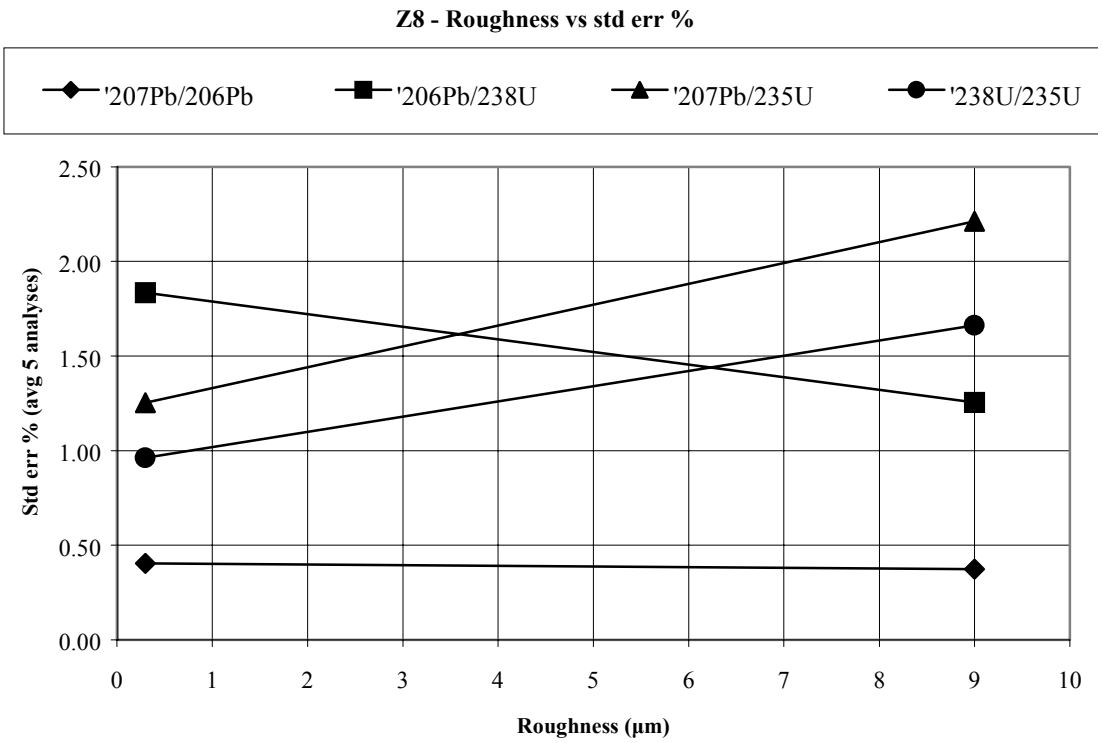

Figure 9.7 - Diagram showing the effect of roughness of the sample surface on the precision of isotopic ratios.

Applications of U-Pb dating by LA-ICPMS

Below we review the few published applications to geological problems and supplement them with work in progress at UQAM's laboratory. We use an excimer 193 nm laser ablation system consisting of the LambdaPhysik Compex 102-ArF laser and a beam delivery system designed by Merchantek-New Wave Research. The laser pulse duration is 25 ns. The laser ablation system is coupled to a multicollector MC-ICPMS IsoProbe from Micromass. Data were acquired in static, multi-collection mode using 6 Faraday collectors, and the only mass configuration array possible due to the large mass spread (~14%) is shown in Table 9.1. Sample analysis consisted of a 50 seconds on-peak baseline measurement prior to the start of laser ablation, followed by two half-mass unit baseline measurements after ablation had commenced. Data acquisition consisted of one block of 50 measurements, each integrated over 1 second. The first few ablation experiments consisted of adjusting the nebuliser gas (Ar) flow rate to the ablation cell so as to obtain the accurate $^{206}Pb/^{238}U$ ratio on the internal standard UQ-Z8 which has been dated by ID-TIMS at

Table 9. 1. Collector array and data analysis structure for in-situ U-Th-Pb isotopic measurements

Faraday Cup Position	Low 3	Low 2	Low 1	Axial Daly	High 1	High 2	High 3	High 4	High 5	High 6
Atomic mass unit	206	207	208	218*				232	235	238
Elements collected	Pb	Pb	Pb					Th	U	U

* Reference mass only used for ion signal centering.

1143±1 Ma (Machado & Gauthier 1996). Age calculations and plotting were done with Isoplot/Ex (Ludwig 2000). No corrections were applied to the data presented here.

One of the great advantages of the method is its high analytical throughput since one analysis takes a few minutes or less. This led to its primary application of dating single detrital zircons because a relatively large number of analyses is required and, generally, the highest precision is not necessary. Published data were obtained either with IR (1064 nm) or UV (266 nm) lasers coupled to ICP-quadropole mass spectrometers and pertain to the analysis of siliciclastic rocks with the aim of unravelling the tectonic significance of sedimentary sequences in orogenic belts (Machado & Gauthier 1996, Machado *et al*. 1996, Scott & Gauthier 1996, Fernández-Suárez *et al*. 2000). If large, macroscopic zircons are available, several analyses can be performed on the same grain and good precisions obtained (Fig. 9.8).

When dating metamorphosed detrital rocks it is desirable to obtain the age of the source rock as well as the age of metamorphism. If detrital zircons lost Pb at the time of metamorphism and/or if they display metamorphic overgrowths, it may be possible to obtain both ages (Fig. 9.9). Metamorphic monazite can also be used to determine the age of metamorphism (Machado & Gauthier 1996). As indicated before, large zircon crystals provide the opportunity to obtain more precise ages (Fig. 9.10)

LA-ICPMS dating of zircon from igneous rocks (Fig. 9.11) allows the determination of the age of crystallization as well as of inheritance if present (Fig. 9.12).

Summary

In only a few years, U-Pb dating by the laser ablation-ICPMS method has evolved from yielding only $^{207}Pb/^{206}Pb$ ages precise to 0.5-6% to the production of $^{206}Pb/^{238}U$ and $^{207}Pb/^{235}U$ ages precise to 0.3-3%. This advance is attributable to the use of deep-UV lasers together with magnetic sector-multicollector mass spectrometers. Isotopic and inter-element biases have been the major hurdles to obtaining precise and accurate ages and, as shown above a number of variables are at play. Different analytical strategies are emerging to control or minimise mass fractionation. The generalization of state-of-the-art instrumentation, in particular the use of 157 nm lasers with ultrashort pulses in the femtosecond range will

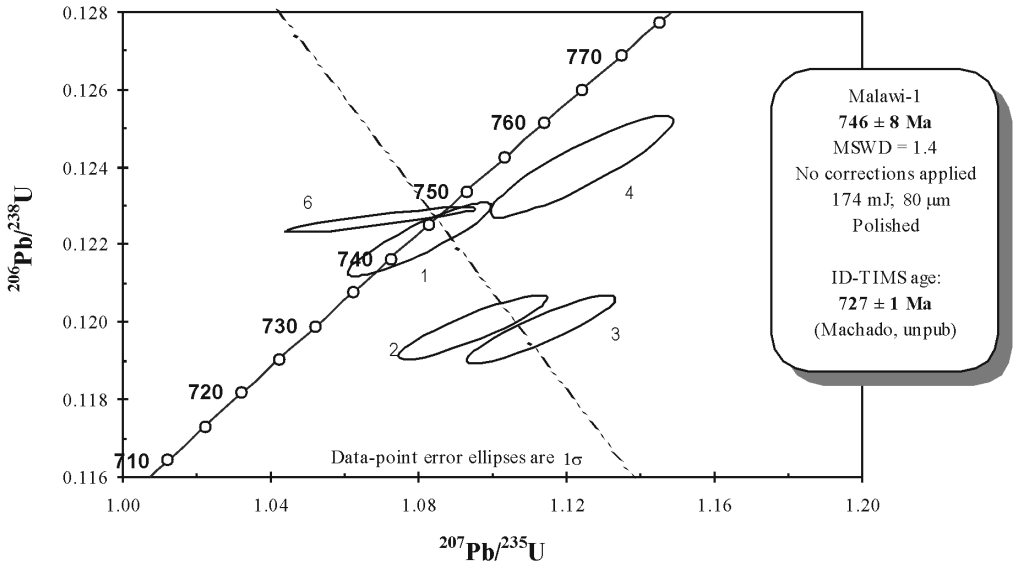

Figure 9.8 - Measured U and Pb isotopic ratios for a macroscopic detrital zircon from Malawi. No corrections applied to the measured ratios. Intercept age calculated with Isoplot (Ludwig 2000). Precision on the age at 2σ.

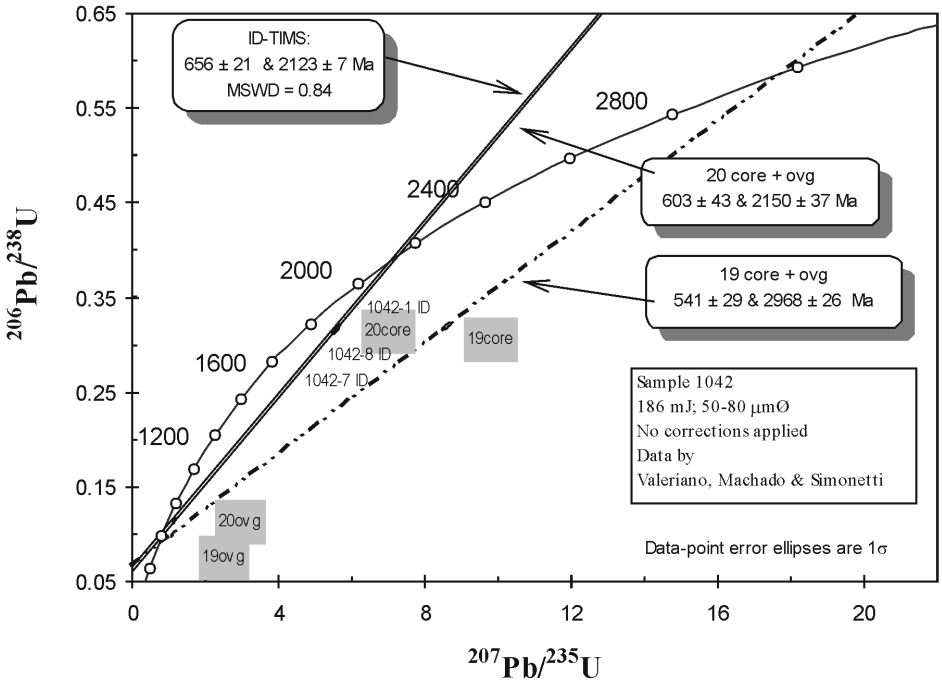

Figure 9.9 - Concordia diagram for zircons from a quartzite from the Araxá Group, Brazil. Three detrital zircons (1042-1, 7 and 8) were analysed by ID-TIMS and define a discordia yielding a metamorphic age of 656±21 Ma. Monazite from this rock is concordant at 602 Ma. LA-ICPMS analyses of core and overgrowth of grain 20 define a discordia line very close to that obtained by the ID-TIMS analyses with a lower intercept at 603 Ma. LA-ICPMS analyses of the core of grain 19 indicate the presence detrital zircons from an Archean source in addition to a Paleoproterozoic one. The lower intercept of the discordia defined by the analysis of the core and the overgrowth is younger than the previous ones at 541 Ma possibly due to Pb loss in the overgrowth (a sector of the laser beam fell outside of the overgrowth). Concordia intercept ages calculated with Isoplot (Ludwig 2000). Precision on the ages is at 2σ.

result in the rapid evolution of the method.

A sign of the infancy of the method is the scarce number of publications relating its applications to geological problems. Unlike U-Pb dating by ID-TIMS, the LA-ICPMS method is well suited to the determination of the age of provenance of detrital rocks and almost all published applications are in this field.

In contrast to Rb-Sr and Sm-Nd dating methods, U-Pb dating does not yield isotopic ratios with petrogenetic information. This has been a considerable disavantage which laser ablation-ICPMS may overcome because it is possible to obtain Hf isotopic ratios on the same zircon crystals dated by U-Pb by the same method.

IN SITU Hf ISOTOPE ANALYSIS OF ZIRCON

Introduction

Lutetium-176 decays by beta emission to hafnium-176 with a half-life of 3.73 ± 0.05 (Dalmasso *et al*., 1992) to 3.69 ± 0.02 billion years (Nir-el and Lavi, 1998). The Lu-Hf isotope system is an important chronometer because a significant amount of the parent isotope still persists today, and the half life is short enough for significant variation to have occurred in the isotopic

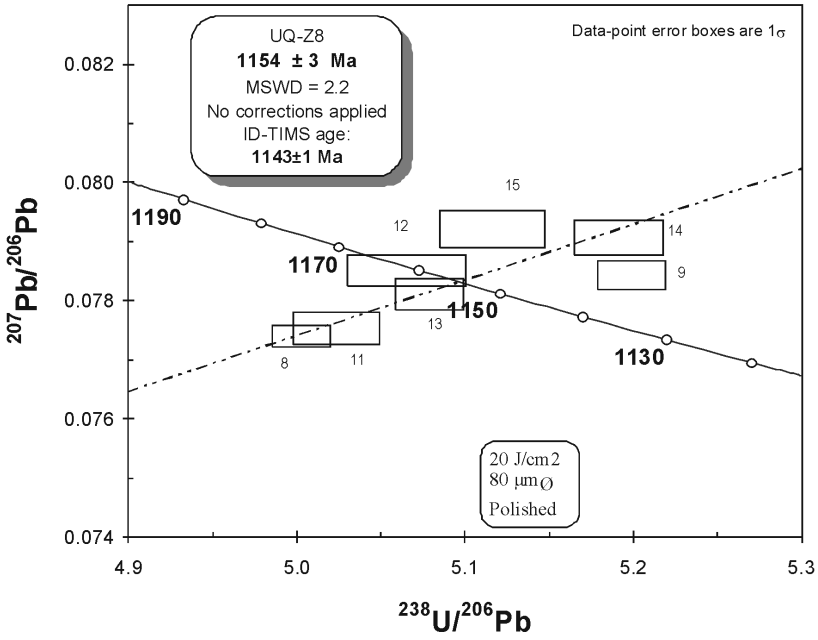

Figure 9.10 - Tera-Wasserburg concordia diagram for macroscopic zircon UQ-Z8. The least magnetic fragments were analysed and they are concordant by ID-TIMS. Concordia intercept ages calculated with Isoplot (Ludwig 2000). Precision on the age is at 2σ.

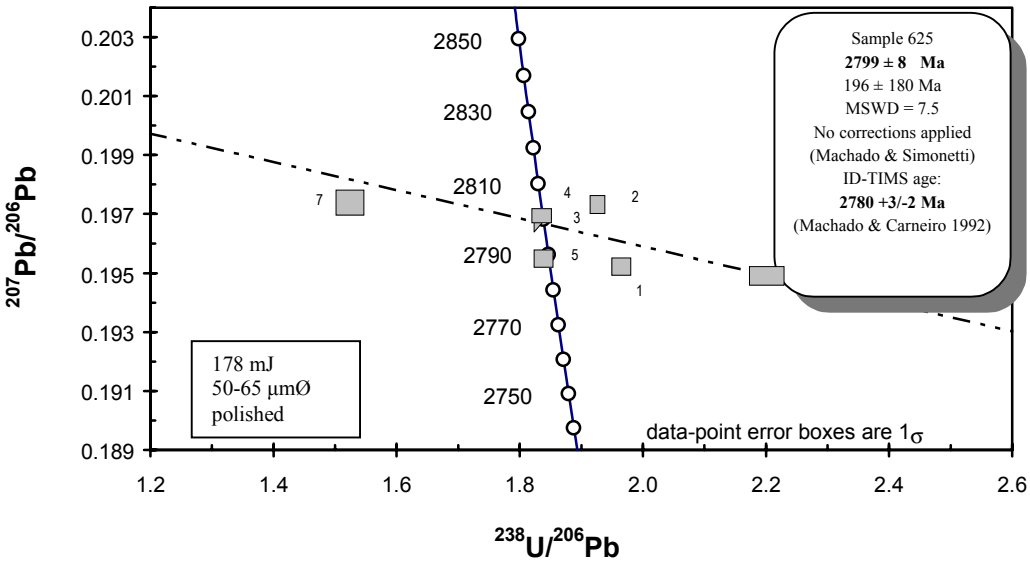

Figure 9.11 - Tera-Wasserburg concordia diagram for zircon from an Archean granodiorite intrusion devoid of inheritance. Concordia intercept ages calculated with Isoplot (Ludwig 2000). Precision on the ages is at 2σ.

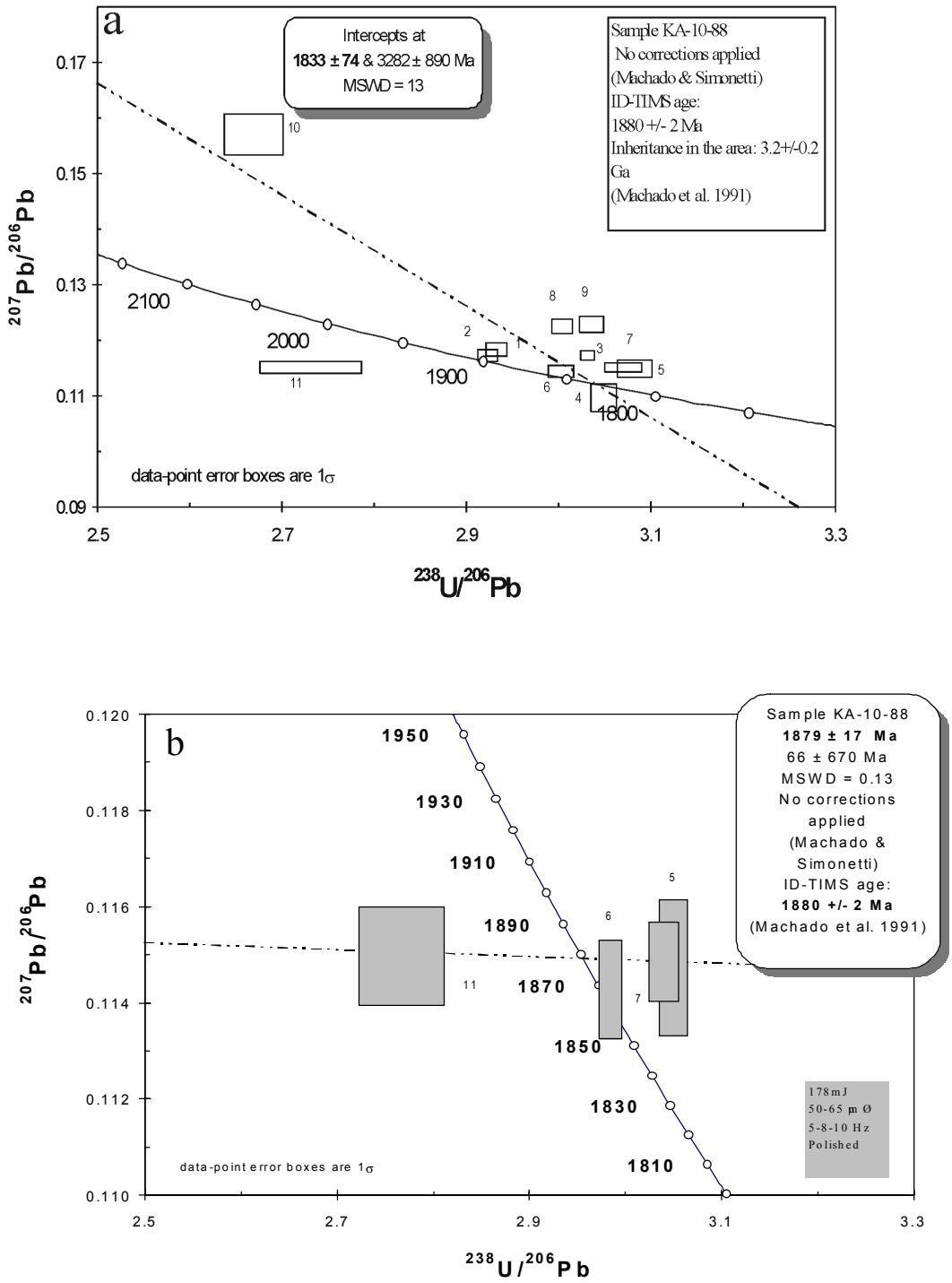

Figure 9.12 a - Tera-Wasserburg concordia diagram for a granodiorite from the Carajás area, Brazil. Inheritance of 3.2 Ga is apparent in agreement with ID-TIMS data (Machado et al. 1991). The lower intercept age is younger but within error of the ID-TIMS age. However, the analyses showing the highest signal intensities yield an age close to the ID-TIMS age, as shown in Figure 9.12 b. Concordia intercept ages calculated with Isoplot (Ludwig 2000). Precision on the ages is at 2σ.

composition of the daughter element. Boudin and Deutsch (1970) were the first to realize the potential of the Lu-Hf isotope system as a chronometer. Unlike the Sm-Nd chronometer, in which both rare earth elements (REE) are characterized by similar chemical properties, Hf (high field strength element; HFSE) exhibits geochemical behavior and mineral/melt partition coefficients that are significantly different from those of Lu (heavy rare earth element; HREE; e.g. Fujimaki *et al*., 1984; Hart and Dunn, 1993). This results in the strong fractionation of parent and daughter element during magmatic and metamorphic processes indicating the important potential of the Lu-Hf isotopic system in geochronology (e.g. Duchêne *et al*., 1997) and as a geological tracer (e.g. Blichert-Toft *et al*., 1997; Scherer *et al*., 2000).

The Lu-Hf systematics of zircon are of particular interest because Hf forms an integral part of the zircon lattice, therefore renders it extremely resistant to metamorphism or erosion, and its age can be precisely determined by U-Pb dating. Zircon is typically characterized by high Hf concentrations (ca. 10000 ppm) and low $^{176}Lu/^{177}Hf$ ratios (usually <0.0005) such that the correction for *in situ* radiogenic growth of ^{176}Hf is negligible. Consequently, these features render zircon ideal for Hf isotope investigations of ancient rocks (>3 Ga old; e.g. Patchett *et al*., 1981; Corfu and Noble, 1992; Vervoort *et al*., 1996; Amelin *et al*., 1999).

Initial $^{176}Hf/^{177}Hf$ ratios are typically expressed in epsilon (ε) notation, which is defined as: $\varepsilon Hf(t) = (^{176}Hf/^{177}Hf_{sample(t)}/^{176}Hf/^{177}Hf_{CHUR(t)} - 1) \times 10^4$, where *(t)* is the geological age of the sample, $^{176}Hf/^{177}Hf_{CHUR(t)}$ is the isotopic composition of the *Ch*ondritic *U*niform *R*eservoir at time *t*. This reservoir is believed to represent the unprocessed material of the early Solar System (primitive, undifferentiated) and has been established with the Lu-Hf isotope systematics of chondrites (class C, O and E meteorites; Blichert-Toft and Albarède, 1997). The temporal variation in $^{176}Hf/^{177}Hf$ ratios of CHUR through geologic time is defined by a $^{176}Lu/^{177}Hf$ value = 0.0332 ± 2 and a present-day $^{176}Hf/^{177}Hf$ = 0.282772 ± 29 (Blichert-Toft and Albarède, 1997). This corresponds to an initial $^{176}Hf/^{177}Hf$ value of 0.279742 ± 29 for Solar System material 4.56 Ga ago. Thus, samples derived from a depleted or enriched (with respect to incompatible elements) source relative to CHUR at time *t* have $\varepsilon Hf_{(t)}$ values that are >0 (positive) and <0 (negative), respectively. The Hf isotopic composition (radiogenic $\varepsilon Hf_{(t)}>0$ or unradiogenic $\varepsilon Hf_{(t)}<0$) of newly formed crust is inherited from its mantle source, and the nature (depleted or enriched) of the latter is dependent upon its precursor evolutionary history (i.e. degree of melt depletion). Based on Hf isotope results from early Archean rocks, a consensus is now emerging which suggests that there is little or no evidence to indicate the presence of a primitive mantle reservoir early in the Earth's history (e.g. Vervoort *et al*., 1996; Vervoort and Blichert-Toft, 1999).

Initial Hf isotope compositions for zircon formed within felsic magmas (i.e. granites) derived from melting of crust reflect the petrogenetic history of their crustal source. Granitic melts formed by the melting of young crust recently formed from depleted mantle (e.g. modern island arc settings) crystallize zircons with radiogenic initial Hf isotopic compositions ($\varepsilon Hf_{(t)}>0$) similar to that of their mantle source. Contrarily, felsic melts derived from melting of reworked, old continental crust generate zircons with unradiogenic initial Hf isotope ratios ($\varepsilon Hf_{(t)}<0$). An important contribution into understanding the evolution of the continental crust has been through the Hf isotopic investigation of Archean detrital zircons, which suggest rapid addition of crustal material between 2.5 and 3.0 Ga ago and this is consistent with models advocating for gradual growth of continental crust (Stevenson and Patchett, 1990).

Early work utilized a chemical separation technique, which allowed the isotopic analysis of Hf by TIMS with relatively good precision so as to apply this radioactive system as a geochemical tracer of igneous processes (Patchett and Tatsumoto 1980a, b, c). Hf isotopic analysis by TIMS, however, required relatively large amounts of sample (microgram level) in order to compensate for the poor ionization efficiency of this element during TIMS analysis. This situation failed to provide external precisions comparable to those obtained for studies using the Sr and Nd isotope systems. The recent introduction of multicollector-inductively coupled plasma mass spectrometers (MC-ICPMS) has made possible the routine, high-precision, high efficiency isotope analysis of Hf (and Lu) on much smaller sample sizes

(<50 ng; Blichert-Toft *et al*. 1997). The main advantage of MC-ICPMS for Hf isotope analysis is the plasma source, which ionizes elements characterized by high ionization potential with much greater efficiency than TIMS while retaining the advantages of conventional mass spectrometry (i.e. magnetic sector, multi-collector configuration). In addition to major technological improvements with regards to isotopic measurements, a straightforward chemical separation technique (two-step ion exchange column chemistry) for Hf and Lu has also been introduced with high efficiency (85% recovery) and low blanks (Blichert-Toft *et al*. 1997). Within the last 3 years, both aspects have combined to produce an explosion of published Hf isotopic studies on a wide variety of geological problems. Some of the important findings that have been reported recently include determination of the planetary reference value for bulk silicate Earth (BSE; Blichert-Toft *et al*., 1997; Blichert-Toft and Albarède, 1997), evidence for the preservation of crust and its subsequent reworking during the Earth's early history (Amelin *et al*., 1999), and the temporal Hf isotopic evolution for depleted mantle (Vervoort and Blichert-Toft, 1999).

Most recently, MC-ICPMS has been combined with laser ablation systems (e.g. 266 nm Nd:YAG; Griffin *et al*. 2000) so as to investigate *in situ* isotopic composition of Hf-rich minerals such as zircon. Thus, providing both the *in situ* Hf isotopic composition and the U-Pb isotope systematics for the same zircon grain (or parts of) renders laser ablation-MC-ICPMS a powerful technique in the field of isotope geochemistry. This combination also obviates one of the main disadvantages of the U-Pb system, which is its deficiency as an isotope tracer for petrogenetic processes.

Analytical procedure

Here we present preliminary results of on-going development related to *in situ* Hf isotopic analyses of zircon at GEOTOP-UQAM. The Hf isotopic data were obtained using the same instrument as indicated above for U-Pb analyses. The laser operating conditions for the Hf experiments consisted of pulse energies of ~150 to 170 mJ (i.e. ~0.15 to 0.17 mJ/pulse), and corresponding energy density of ~16.5 to 18.7 J/cm^2 at the sample surface. The repetition rate was 10 Hz and the predominant spot size used was 50 µm, except for zircon 91500, which was analyzed with a 80 µm beam.

The Hf isotopic data were acquired in static, multicollection mode using 9 Faraday collectors, and the mass configuration array is shown in Table 9.2. Prior to laser ablation, a 50 ppb solution of the standard JMC 475 was aspirated into the ICP source using an Aridus® microconcentric nebuliser at an uptake rate of ~50 µl/minute and analysed for ~10 minutes. This corresponds to approximately 25 ng of total Hf consumed per analysis, and the results from repeated measurements (n=40) of the JMC 475 standard over the last six months (encompassing the period for this study) are shown in Table 9.3. All of the Hf isotopic measurements listed show excellent reproducibility, and are all identical (within error) to their accepted values (Blichert-Toft et al. 1997). Moreover, the "sample-out" line from the Aridus® was ("y-") connected to the "sample-out" line from the laser ablation cell just outside the torch box. This set-up enables to evaluate the mass bias induced during the ablation process, since after exiting the laser ablation cell both particulate and liquid aerosols travel along the same tubing before entering the ICP torch.

Table 9.2 . Collector array and data analysis structure for in-situ Hf isotopic measurements

Faraday Cup Position	Low 3	Low 2	Axial	High 1	High 2	High 3	High 4	High 5	High 6
Atomic mass unit collected	172	173	175	176	177	178	179	180	182
Elements collected	Yb monitor	Yb	Lu monitor	Hf with Lu and Yb interferences	Hf	Hf	Hf	Hf with W interferences	W monitor

Table 9.3 . Analyses of Hf standards

Standard	$^{176}Lu/^{177}Hf$	$^{176}Yb/^{177}Hf$	$^{176}Hf/^{177}Hf$	$^{178}Hf/^{177}Hf$	$^{180}Hf/^{177}Hf$
Solution mode:					
JMC 475 (n=40; 50 ppb)	---	---	0.282159 ±0.000033	1.46733 ±0.00012	1.88680 ±0.00030
JMC 475 –1 (+Lu +Yb; n=4)	0.000724 ±0.000004	0.130833 ±0.000990	0.282153 ±0.000055	1.46738 ±0.00004	1.88704 ±0.00011
JMC 475 –2 (+Lu +Yb; n=4)	0.002861 ±0.000018	0.091587 ±0.000667	0.282135 ±0.000030	1.46740 ±0.00003	1.88696 ±0.00012
Laser Ablation:					
Zircon 91500 (n=5; this study)	0.000308 ±0.000034	0.008798 ±0.002032	0.282270 ±0.000123	1.46746 ±0.00014	1.88649 ±0.00048
Zircon 91500 LA-MC-ICP-MS (n=60)[a]	0.000295 ±0.000050		0.282297 ±0.000044	1.46716 ±0.00017	
Zircon 91500 TIMS (n=7)[b]	0.000288 ±0.000014		0.282284 ±0.000003	1.46714 ±0.00001	

All errors represent 2σ standard deviations. **a**: Data from Griffin et al. (2000); **b**: Data from Wiedenbeck et al. (1995)); ---: Ion beam signals of Lu and Yb are essentially nil for the JMC 475 standard. Hf isotopic ratios are normalized to $^{179}Hf/^{177}Hf = 0.7325$.

Mass Bias

Mass bias (or fractionation) is calculated by directly comparing the value of an isotopic ratio, which is known and constant throughout the Earth, to the same ratio measured during a mass spectrometric analysis (TIMS or ICP-MS). During an ICP-MS analysis, the abundance sensitivity of two isotopes for the same element is different, such that the lighter ions are less efficiently transmitted. This feature may be attributed to either "space charge" effects in the ICP (Maréchal *et al*., 1999) or in the region of the skimmer cone (Walder *et al*., 1997). The correction for mass bias has been described using various equations, such as the linear or power laws, both of which assume that the fractionation is proportional to the mass difference only. However, the exponential law defines the fractionation as also being mass dependent, and it has been well established from previous studies (e.g. Blichert-Toft *et al*. 1997) that mass bias on the MC-ICP-MS is best monitored using the exponential law (Russell *et al*. 1978). This law is expressed as follows:

$$R_{true} = R_{measured}(M_2/M_1)^f$$

where R is the ratio of the ion beams at masses M_2 and M_1. The variable f is the mass discrimination coefficient (also referred to as the Beta factor). In the case of Hf, measured isotopic ratios are normalized to $^{179}Hf/^{177}Hf = 0.7325$, which typically results in mass bias corrections of ~1.1% amu^{-1} (per atomic mass unit). Mass fractionation for MC-ICPMS is therefore approximately one order of magnitude larger than for TIMS. A comparison between the measured $^{179}Hf/^{177}Hf$ ratios obtained here in solution mode to those recorded during laser ablation yield a similar range of values on a daily basis (total variation <0.2% in ablation mode).

Contrary to solution mode analysis in

which samples have undergone a chemical separation procedure for Hf and Lu (+Yb), *in situ* determination by laser ablation-MC-ICP-MS of zircon measures the ion signals from these three elements simultaneously. It becomes imperative, therefore, to determine accurate corrections for ^{176}Lu and ^{176}Yb interferences on ^{176}Hf (Table 9.2). This is achieved by using the intensities of the measured ^{175}Lu and $^{173(or\ 172)}$Yb and applying an appropriate mass bias correction in order to determine the correct amount of ^{176}Lu and ^{176}Yb. Solutions produced from high purity metals of Lu and Yb from the Ames Laboratory (20 and 10 ppb, respectively) were also aspirated into the ICP source in order to determine the mass bias (exponential law) used for the respective interference corrections of ^{176}Lu and ^{176}Yb on ^{176}Hf (Table 9.2). The mass bias for Lu was determined by measuring the ^{176}Lu/^{175}Lu ratio and comparing the results to the recommended value of 0.02656 (Blichert-Toft *et al*. 1997). Similarly, the mass bias for Yb was measured using the ^{176}Yb/^{173}Yb ratio and using the recommended value of 0.78761 (Blichert-Toft *et al*. 1997). As an internal check, the calculated Beta factor was applied to the measured ^{173}Yb/^{172}Yb ratio to verify that the mass bias corrected value for the latter is 0.73690 (Blichert-Toft *et al*. 1997).

A series of Lu- and Yb-doped JMC 475 solutions were prepared in order to test the established Lu- and Yb-interference correction procedures for *in situ* laser ablation of zircon, an approach similar to that used by Griffin *et al*. (2000). Table 9.3 lists the Hf isotopic data from eight such solutions, along with their calculated ^{176}Lu/^{177}Hf and ^{176}Yb/^{177}Hf ratios. Comparison of the latter two ratios to those found in naturally occurring zircons (e.g. Table 9.4) indicate that the former are clearly much higher (one order of magnitude for ^{176}Yb/^{177}Hf). This was purposely done in order to test the interference corrections for ^{176}Lu and ^{176}Yb in extreme situations. The Hf isotopic data for the Lu- and Yb-doped JMC 475 solutions (Table 9.3) are virtually identical (certainly within error) of the recommended values and thus confirm the accuracy of the interference corrections. Subsequent to the analysis of the various standards in liquid mode, nebuliser and sweep gas rates to both the Aridus® and ablation cell were adjusted in order to maximize the ion beam intensity during ablation. Typical flow rates of the ablation cell gas (Ar) varied between 0.2 to 0.4 l/minute.

Results

Total Hf ion beam intensities varied between 0.5 to 2.0x 10^{-11} A, depending on the experimental conditions and the Hf contents of the zircons. This range in ion beam intensity is similar to that obtained on megacryst zircons from various kimberlites worldwide (Griffin *et al*. 2000); however the latter were obtained using 80 µm spot sizes (vs. 50 µm in this study). Sample analysis consisted of a 50 seconds on-peak baseline measurement prior to the start of laser ablation, and followed by two half-mass unit baseline measurements after ablation had commenced. Data acquisition consisted of 50 measurements, each integrated over 2 seconds yielding typical internal precisions of 0.014 to 0.03% (2σ) on the ^{176}Hf/^{177}Hf ratio. These errors are clearly much lower than the whole range of Hf isotopic compositions defined by the different zircon samples listed in Table 9.4.

Zircon 91500

Analyses of this zircon by ID-TIMS has been reported by Wiedenbeck *et al*. (1995) and is listed in Table 9.3. In addition, LA-MC-ICP-MS (266 nm Nd:YAG + NU Plasma) analyses of the same zircon (Griffin *et al*. 2000) are also included for comparative purposes in Table 9.3. Griffin *et al*. (2000) have described this zircon as reliable standard material since it is quite homogeneous in terms of Yb and Lu contents, as well as the ^{176}Hf/^{177}Hf isotopic composition. However, they do state that their observed range of ^{176}Hf/^{177}Hf ratios exceeds three times the standard deviation of the mean, suggestive of slight isotopic heterogeneity (Griffin *et al*. 2000). The range of ^{176}Hf/^{177}Hf values obtained here on five analyses is approximately twice that of the standard deviation of the mean. Compared to the Hf isotopic data obtained by both TIMS and laser ablation-ICP-MS for zircon 91500, the results from this study yield similar values (Table 9.3). In addition, as a first approximation we have calculated the ^{176}Lu/^{177}Hf and ^{176}Yb/^{177}Hf ratios using the measured intensities of ^{180}Hf, ^{175}Lu, and ^{173}Yb and applied the respective mass bias determined from the various standards analysed in solution mode. The fact that the ^{176}Lu/^{177}Hf

Table 9.4. *In situ* Hf isotopic composition of zircons

Sample		$^{176}Lu/^{177}Hf$	$^{176}Yb/^{177}Hf$	$^{176}Hf/^{177}Hf$ ±2σE	$^{178}Hf/^{177}Hf$ ±2σE	$^{180}Hf/^{177}Hf$ ±2σE	ε $Hf_{(T)}$
UQ-Z8:							
(1143 Ma)	1	0.00076	0.02803	0.28235 ±09	1.46777 ±16	1.88719 ±44	10.8
	2	0.00086	0.03079	0.28252 ±10	1.46734 ±12	1.88820 ±37	16.8
	3	0.00030	0.00986	0.28198 ±09	1.46720 ±11	1.88629 ±60	-2.1
	4	0.00041	0.01501	0.28252 ±11	1.46703 ±16	1.88626 ±43	16.9
	5	0.00037	0.01376	0.28205 ±11	1.46751 ±15	1.88735 ±63	0.5
	6	0.00038	0.01286	0.28249 ±09	1.46746 ±13	1.88719 ±39	15.8
	7	0.00076	0.02573	0.28236 ±04	1.46739 ±06	1.88644 ±20	11.2
	8	0.00074	0.02451	0.28235 ±03	1.46733 ±06	1.88634 ±15	10.5
	9	0.00029	0.00983	0.28219 ±04	1.46737 ±07	1.88639 ±26	5.3
	10	0.00040	0.01453	0.28228 ±05	1.46744 ±08	1.88645 ±30	8.7
Average[a]:		0.00053	0.01849	0.28231 ±36	1.46738 ±37	1.88681 ±123	
Malawi:							
(727 Ma)	1	0.00013	0.00393	0.28221 ±13	1.46665 ±17	1.88601 ±57	-3.3
	2	0.00056	0.01694	0.28259 ±10	1.46741 ±16	1.88697 ±48	10.0
	3	0.00056	0.01390	0.28233 ±07	1.46762 ±10	1.88655 ±32	0.8
	4	0.00072	0.01958	0.28229 ±07	1.46768 ±14	1.88694 ±34	-0.8
	5	0.00098	0.03140	0.28214 ±09	1.46745 ±11	1.88706 ±25	-6.1
	6	0.00035	0.00939	0.28232 ±06	1.46746 ±11	1.88670 ±34	0.6
Average[a]:		0.00055	0.01586	0.28231 ±28	1.46738±68	1.88671 ±71	
Peixe:							
(2000 Ma)	1	0.00113	0.03088	0.28149 ±04	1.46739 ±09	1.88641 ±34	-0.7
	2	0.00111	0.03155	0.28163 ±05	1.46746 ±09	1.88630 ±44	4.3
	3	0.00110	0.02982	0.28157 ±05	1.46743 ±09	1.88673 ±36	2.0
	4	0.00110	0.03471	0.28146 ±06	1.46755 ±09	1.88662 ±48	-1.7
	5	0.00113	0.02974	0.28160 ±06	1.46750 ±08	1.88710 ±28	3.3
	6	0.00110	0.03404	0.28149 ±08	1.46732 ±12	1.88685 ±49	-0.7
	7	0.00116	0.03125	0.28165 ±04	1.46747 ±09	1.88737±31	5.0
	8	0.00104	0.02686	0.28172 ±05	1.46738 ±10	1.88746 ±29	7.6
	9	0.00103	0.02955	0.28160 ±04	1.46724 ±08	1.88709 ±19	3.4
Average[a]:		0.00110	0.03093	0.28158 ±16	1.46741 ±18	1.88688 ±77	
98-98-95:							
(1750 Ma)	1	0.00025	0.00598	0.28169 ±11	1.46736 ±12	1.88667 ±38	2.8
	2	0.00019	0.00410	0.28160 ±06	1.46757 ±09	1.88749 ±27	-0.2
	3	0.00018	0.00484	0.28204 ±09	1.46727 ±17	1.88617 ±47	15.6
	4	0.00036	0.00782	0.28199 ±08	1.46706 ±09	1.88629 ±28	13.5
	5	0.00032	0.00698	0.28178 ±07	1.46718 ±10	1.88669 ±31	6.2
	6	0.00021	0.00472	0.28172 ±09	1.46741 ±15	1.88649 ±34	3.9
Average[a]:		0.00025	0.00574	0.28180 ±32	1.46731 ±32	1.88663 ±85	

Table 9.4(cont'd). *In situ* Hf isotopic composition of zircons

Sample		$^{176}Lu/^{177}Hf$	$^{176}Yb/^{177}Hf$	$^{176}Hf/^{177}Hf$ ±2σE	$^{178}Hf/^{177}Hf$ ±2σE	$^{180}Hf/^{177}Hf$ ±2σE	ε $Hf_{(T)}$
KA-11-88:							
(~3.0 Ga)	1	0.00067	0.02072	0.28116 ±05	1.46720 ±09	1.88643 ±32	11.8
	2	0.00040	0.01188	0.28104 ±06	1.46773 ±11	1.88704 ±31	8.1
	3	0.00045	0.01154	0.28094 ±06	1.46725 ±11	1.88658 ±37	4.2
	4	0.00070	0.02060	0.28116 ±07	1.46725 ±08	1.88670 ±19	11.5
Average[a]:		0.00046	0.01342	0.28108 ±19	1.46736 ±43	1.88669 ±45	
M94-C1:							
(~3.5 Ga)	1	0.00052	0.01665	0.28099 ±07	1.46748 ±11	1.88668 ±28	17.9
	2	0.00045	0.01336	0.28056 ±07	1.46760 ±11	1.88635 ±23	2.7
	3	0.00045	0.01429	0.28028 ±08	1.46771 ±16	1.88686 ±34	-7.3
	4	0.00033	0.01212	0.28013 ±13	1.46718 ±16	1.88601 ±55	-12.4
Average[a]:		0.00044	0.01410	0.28049 ±66	1.46749 ±39	1.88648 ±65	
M93-02:							
(2900 Ma)	1	0.00108	0.02950	0.28100 ±07	1.46747 ±12	1.88676 ±45	2.8
	2	0.00129	0.03829	0.28125 ±06	1.46735 ±11	1.88665 ±40	11.0
Average:		0.00119	0.03390	0.28112	1.46741	1.88671	
1592:							
(3500 Ma)	1	0.00069	0.02027	0.28064 ±06	1.46748 ±10	1.88637 ±32	5.0
	2	0.00057	0.01650	0.28079 ±06	1.46748 ±12	1.88664 ±38	10.5
	3	0.00060	0.01704	0.28065 ±06	1.46741 ±14	1.88601 ±48	5.7
	4	0.00092	0.03063	0.28088 ±07	1.46738 ±12	1.88605 ±38	13.0
Average[a]:		0.00069	0.02111	0.28074 ±20	1.46744±09	1.88627 ±51	
3331:							
(3500 Ma)	1	0.00093	0.03264	0.28094 ±20	1.46769 ±20	1.88683 ±20	14.9
	2	0.00090	0.03241	0.28087 ±20	1.46766 ±20	1.88643 ±20	12.5
	3	0.00106	0.02963	0.28101 ±20	1.46714 ±20	1.88676 ±20	17.2
Average[a]:		0.00096	0.03156	0.28094 ±12	1.46750 ±50	1.88667 ±34	
2274:							
(2800 Ma)	1	0.00119	0.04712	0.28150 ±09	1.46726 ±13	1.88650 ±44	18.0
	2	0.00042	0.01467	0.28104 ±13	1.46722 ±21	1.88746 ±69	3.3
Average:		0.00081	0.03089	0.28127	1.46724	1.88698	

a: Uncertainties associated with average values represent 2σ standard deviations.

calculated here is in agreement with the previously published values (i.e. Wiedenbeck *et al*. 1995; Griffin *et al*. 2000; Table 9.3) lends support to the method used in this study. Moreover, no correlation was observed between calculated $^{176}Lu/^{177}Hf$ or $^{176}Yb/^{176}Hf$ and corrected $^{176}Hf/^{177}Hf$ ratios for zircon 91500 and the other samples analysed (Fig. 9.13) lending additional support to the accuracy of the results listed in Table 9.3. Thus, the results obtained for zircon 91500 suggest that the *in situ* Hf isotopic analyses obtained in this study are reliable.

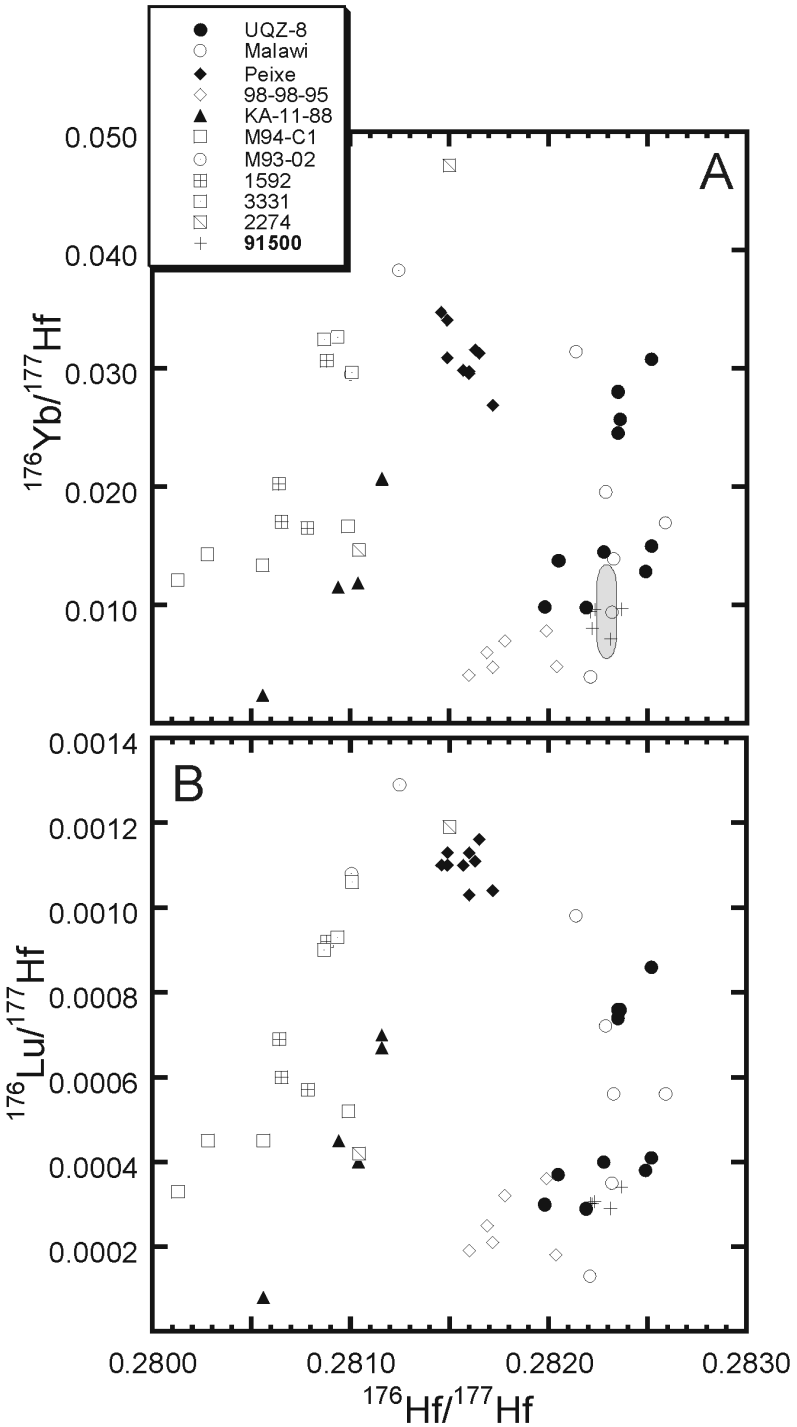

Fig. 9.13. (A) $^{176}Yb/^{177}Hf$ vs. and (B) $^{176}Lu/^{177}Hf$ vs. $^{176}Hf/^{177}Hf$ for zircon 91500 and other samples analysed in this study. The elipse in (A) represents range of analyses for zircon 91500 obtained by Griffin et al. (2000), and these are in agreement with the results obtained in this study.

Samples

In situ Hf isotopic compositions for various zircons representing a wide spectrum of ages are listed in Table 9.4. The $^{176}Hf/^{177}Hf$ isotope ratios shown in Fig. 9.14 are corrected for *in situ* growth of ^{176}Hf using the calculated $^{176}Lu/^{177}Hf$ ratios (Table 9.4) and previously determined U-Pb ages; however, the age correction for *in situ* decay of ^{176}Lu can be considered negligible (typically 0.00001 to 0.00002) for most of the zircons listed in Table 9.4 due to their low $^{176}Lu/^{177}Hf$ ratios. ε_{Hf} values were calculated using the chondritic values of Blichert-Toft and Albarède (1997), whereas evolution of the depleted mantle source was calculated using an initial $^{176}Hf/^{177}Hf$ value of 0.279718 (4.56 Ga ago) and a $^{176}Lu/^{177}Hf$ of 0.0378. This results in a present-day $^{176}Hf/^{177}Hf$ ratio for depleted mantle of ~0.28320 similar to that of average MORB (e.g. Griffin *et al*. 2000).

Most of the Hf isotopic data for the zircons plot between the evolution lines for CHUR and depleted mantle with the exception of those from Malawi (Fig. 9.14). These seem to have been derived from a much less radiogenic source (crustal) compared to the remaining zircons. Moreover, some of the Archean zircons (e.g. 2274) display Hf isotopic compositions too radiogenic for their age. As the unit containing them was metamorphosed to amphibolite facies, it is possible that metamorphism disturbed the Lu-Hf systematics. Somewhat problematical are the extremely unradiogenic Hf isotope compositions for zircons from sample M94-C1 at approximately 3.5 Ga (Fig. 9.14). As well, zircon UQ-Z8 (Machado and Gauthier 1996) shows a significant range in Hf isotopic compositions, whereas those for sample Peixe are more tightly constrained. In summary, the zircon data shown in Fig. 9.13 obtained by laser ablation-MC-ICP-MS is reliable, and the method is promising for future use in geochronological and provenance studies for detrital zircons.

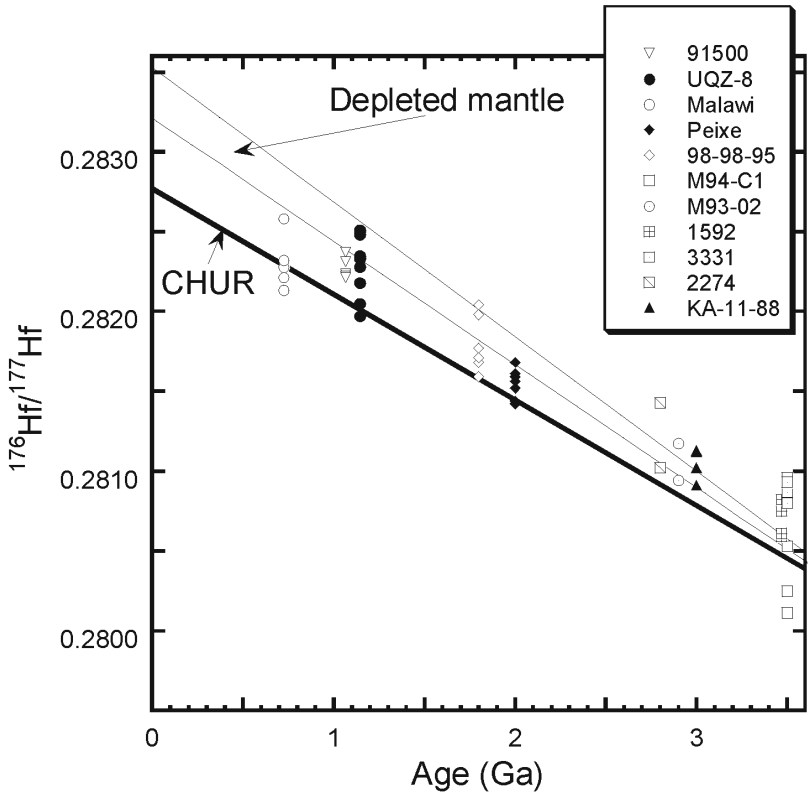

Fig 14. Plot of initial $^{176}Hf/^{177}Hf$ vs. their U-Pb formation age for zircons analysed in this study. The latter were obtained by either TIMS and/or LA-MC-ICP-MS.

SUMMARY AND CONCLUSIONS

A review of the state of the art in U-Pb dating and determination of Hf isotopic ratios on zircon by LA-ICPMS reveals the latter method is closer to standardization of analytical procedures than the former. This is to be expected since Hf has stable isotopes that can be used to monitor and correct for mass fractionation, and also because the Lu content of zircon is low enough to not require a significant age correction of the measured $^{176}Hf/^{177}Hf$. This review also shows that although the U-Pb method still has to solve the problem of elemental-isotopic fractionation, most variables have been identified and current research will overcome it.

Above all, this review shows the exciting possibilities offered by the LA-ICPMS methodology to obtain ages and Hf isotopic characteristics of single zircon crystals.

ACKNOWLEDGEMENTS

The Micromass Isoprobe instrument and the LambdaPhysik-Merchantek-New Wave laser system were financed through NSERC with contributions from FCAR (Québec) and Fondation UQAM. The laboratory is maintained in part with a NSERC MFA grant. We thank C. Gariépy for making the laboratory a reality. J. Visser (Merchantek-New Wave Research) and R. Lapointe have provided technical support. We thank C. Valeriano (UERJ, Brazil) for stimulating discussions, comments on this work and the inclusion of unpublished data, and Dr. J. Košler for critical comments on an earlier version of the manuscript.

REFERENCES

AMELIN, Y., LEE, D.-C., HALLIDAY, A.N. & PIDGEON, R.T. (1999). Nature of the Earth's earliest crust from hafnium isotopes in single detrital zircons. *Nature* **399**, 252-255.

ARROWSMITH, P. (1990): Applications of laser ablation: elemental analysis of solids by secondary plasma mass spectrometry. *In* Lasers and Mass Spectrometry, (David M. Lubman, ed.). Oxford Series on Optical Sciences, Oxford University Press, 179-204.

BLICHERT-TOFT J. & *ALBARÈDE* F. (1997): The Lu-Hf isotope geochemistry of chondrites and the evolution of the mantle-crust system. *Earth and Planet. Sci. Lett.* **148**: 243-258.

BLICHERT-TOFT, J., CHAUVEL, C. & ALBARÈDE F. (1997): Separation of Hf and Lu for high-precision isotope analysis of rock samples by magnetic sector-multiple collector ICP-MS. *Contrib. Mineral. Petrol*. **127**: 248-260.

BOUDIN, A. & DEUTSCH, S. (1970): Geochronology: recent development in the lutetium-176/hafnium-176 dating method. *Science* **168**, 1219-1220.

CHENERY, S., HUNT, A. & THOMPSON, M. (1992): Laser ablation of minerals and chemical differentiation of the ejecta. *J. An. Atom. Spectrom.* **7**, 647-652.

COMPSTON, W., WILLIAMS, I.S. & MEYER, C. (1984): U-Pb geochronology of zircons from lunar breccia 73217 using a sensitive high mass-resolution ion microprobe. *J. Geophys. Res*. **89**, B525-B534.

CORFU, F. & NOBLE, S.R. (1992). Genesis of southern Abitibi greenstone belt, Superior Province, Canada: Evidence from Hf isotope analyses using a single filament technique. *Geochim. Cosmochim. Acta* **56**, 2081-2097.

DALMASSO, J., BARCI-FUNEL, G. & ARDISSON, G.J. (1992). Reinvestigation of the decay of the long-lived odd-odd ^{176}Lu nucleus. *Appl. Radiat. Isot*. **43**, 69-76.

DUCHÊNE, S., BLICHERT-TOFT, J., LUAIS, B., TÉLOUK, P., LARDEAUX, J.-M. & ALBARÈDE, F. (1997). The Lu-Hf dating of garnets and the ages of the Alpine high-pressure metamorphism. *Nature* **387**, 586-589.

DULEY, W.W. (1996): *UV Lasers: effects and applications in materials science*. Cambridge University Press.

EGGINS, S.M., KINSLEY, L.P.J. & SHELLEY, J.M.G. (1998). Deposition and element fractionation processes during atmospheric pressure laser ablation sampling for analysis by ICP-MS. *Applied Surface Science* **127**, 278-286.

FENG, R., MACHADO, N. & LUDDEN, J. (1993). Lead geochronology of zircon by laserprobe-inductively coupled plasma mass spectrometry (LP-ICPMS). *Geochim. Cosmochim. Acta* **57**, 3479-3486.

FERNÁNDEZ-SUÁREZ, J., GUTIERREZ, A.G., JENNER, G.A. & TUBRETT, M.N. (1999). Crustal sources in lower Paleozoic rocks from NW Iberia: insights from laser ablation U-Pb ages of detrital zircons. *J. Geol. Soc.* **156**, 1065-1068.

FERNÁNDEZ-SUÁREZ, J., GUTIÉRREZ-ALONSO, G., JENNER, G.A. & TUBRETT, M.N. (2000). New ideas on the Proterozoic-Early Paleozoic evolution of NW Iberia: insights from U-Pb detrital zircon ages. *Precamb. Res.* **102**, 185-206.

FIGG, D. & KAHR, M.S. (1997): Elemental fractionation of glass using laser ablation inductively coupled plasma mass spectrometry. *Appl. Spectroscopy* **51**, 1185-1192.

FIGG, D., CROSS, J.B. & BRINK, C. (1998): More investigations into elemental fractionation resulting from laser ablation-inductively coupled plasma-mass spectrometry on glass samples. *Appl. Surf. Sci.* **127-129**, 287-291.

FRYER, B.J., JACKSON, S.E. & LONGERICH, H.P. (1993): The application of laser ablation microprobe-inductively coupled plasma-mass spectrometry (LAM-ICP-MS) to *in situ* (U)-Pb geochronology. *Chem. Geol.* **109**, 1-8.

FRYER, B.J., JACKSON, S.E. & LONGERICH, H.P. (1995): Design, operation and role of the laser ablation-microprobe coupled with an inductively coupled plasma mass spectrometer (LAM-ICPMS) in the Earth Sciences. *Can. Mineral.* **33**, 303-312.

FUJIMAKI, H., TATSUMOTO, K.I. & AOKI, K.I. (1984). Partition coefficients of Hf, Zr, and REE between phenocrysts and groundmasses. *J. Geophys. Res.* **89**, B662-B672.

GEERTSEN, C., BRIAND, A., CHARTIER, F., LACOUR, J.-L., MAUCHIENT, P. & SJÖSTROM, S. (1994): Comparison between infrared and ultraviolet laser ablation at atmospheric pressure – implications for solid sampling inductively coupled plasma spectrometry. *J. An. At. Spectrom.* **9**, 17-22.

GRIFFIN, W.L., PEARSON, N.J., BELOUSOVA, E., JACKSON, S.E., VAN ACHTERBERGH, E., O'REILLY, S.Y. & SHEE, S.R. (2000): The Hf isotope composition of cratonic mantle: LAM-MC-ICPMS analysis of zircon megacrysts in kimberlites. *Geochim. Cosmochim. Acta* **64**: 133-147.

GÜNTHER, D., FRISCHKNECHT, R., HEINRICH, C. & KAHLERT, H-J (1997): Capabilities of an argon fluoride 193 nm excimer laser for laser ablation inductively coupled plasma mass spectrometry microanalysis of geological materials. *J. Anal. At. Spectrom.* **12**, 939-944.

GÜNTHER, D. & HEINRICH, C. (1999): Comparison of the ablation behaviour of 266 nm Nd:YAG and 193 nm ArF excimer lasers for LA-ICP-MS analysis. *J. Anal. At. Spectrom.* **14**, 1369-1374.

HART, S.R. & DUNN, T. (1993). Experimental clinopyroxene-melt partitioning of 24 trace elements. *Contrib. Mineral. Petrol.* 113, 1-8.

HIRATA, T. & NESBITT, R.W. (1995): U-Pb isotope geochronology of zircon: evaluation of the laser probe-inductively coupled plasma mass spectrometry technique. *Geochim. Cosmochim. Acta* **59**, 2491-2500.

HORN, I., RUDNICK, R.L. & MCDONOUGH, W.F. (2000). Precise elemental and isotope determination by simultaneous solution nebulization and laser ablation-ICP-MS: application to U-Pb geochronology. *Chem. Geol.* **164**, 281-301.

HORSTWOOD, M., PARRISH, R., NOWELL, G. & NOBLE, S. (2000). Further advances in U-Th-Pb LA-PIMMS. *J. Conference Abstracts* **5**, 532.

KROGH, T.E. (1973): A low-contamination method for hydrothermal decomposition of zircon and extraction of U and Pb for isotopic age determination. *Geochim .Cosmochim. Acta* **37**, 485-494.

KROGH, T.E. (1982a): Improved accuracy of U-Pb zircon dating by selection of more concordant fractions using a high gradient magnetic separation technique. *Geochim. Cosmochim. Acta* **46**, 631-635.

KROGH, T.E. (1982b): Improved accuracy of U-Pb zircon ages by the creation of more concordant systems using an air abrasion technique. *Geochim. Cosmochim. Acta* **46**, 637-649.

KRÖNER, A., O'BRIEN, P.J., NEMCHIN, A. A. & PIDGEON, R. T. (2000): Zircon ages for high pressure granulites from South Bohemia, Czech Republic, and their connection of Carboniferous high temperature processes. *Contrib. Mineral. Petrol.* **138**, 127-142.

LONGERICH, H.P., GÜNTHER, D. & JACKSON, S.E. (1996): Elemental fractionation in laser ablation inductively coupled plasma spectrometry. *Fresenius J. Anal. Chem.* **355**, 538-542.

LUDWIG, K.L. (2000): *Users manual for Isoplot/Ex v. 2.3. A geochronological toolkit for Microsoft Excel.* Berkeley Geochronology Center Sp. Pub. No. 1a. Berkeley, California.

MACHADO, N. & SIMONETTI, A. (2001): Parameters affecting U-Th-Pb elemental-isotopic fractionation in zircon dating by Excimer laser ablation-ICPMS. GAC-MAC, St. John's 2001.

MACHADO, N. & GAUTHIER, G. (1996): Determination of $^{207}Pb/^{206}Pb$ ages on zircon and monazite by laser ablation ICPMS and application to a study of sedimentary provenance and metamorphism in southeastern Brazil. *Geochim. Cosmochim. Acta* **60**: 5063-5073.

MACHADO, N. & CARNEIRO, M. (1992): U-Pb evidence of late Archean tectono-thermal activity in the southern São Francisco shield, Brazil. *Can. J. Earth Sci.* **29**, 2341-2346.

MACHADO, N. LINDENMAYER, Z., KROGH, T.E. & LINDENMAYER, D. (1991): U-Pb geochronology of Archean magmatism and basement reactivation in the Carajás area, Amazon shield, Brazil. *Precamb. Res.* **49**, 329-354.

MACHADO, N., SCHRANK, A., NOCE, C.M. & GAUTHIER, G. (1996): Ages of detrital zircon from Archean-Paleoproterozoic sequences: implications for greenstone belt setting and evolution of a Transamazonian foreland basin in Quadrilátero Ferrífero, southeast Brazil. *Earth Planet. Sci. Letters* **141**, 259-276.

MARÉCHAL, C.N., TÉLOUK, P. & ALBARÈDE, F. (1999). Precise analysis of copper and zinc isotopic compositions by plasma-source mass spectrometry. *Chem. Geol.* **156**, 251-273.

NIR-EL, Y. & LAVI, N. (1998). Measurement of the half-life of ^{176}Lu. *Appl. Radiat. Isot.* **49**, 1653-1655.

OUTRIDGE, P.M., DOHERTY, W. & GREGOIRE, D.C. (1997): Ablative and transport fractionation of trace elements during laser sampleing of glass and copper. *Spectrochim. Acta* **B52**, 2093-2102.

PARRISH, R.R. (1987): An improved micro-capsule for zircon dissolution in U-Pb geochronology. *Chem. Geol.* **66**, 99-102.

PARRISH, R.R. & KROGH, T.E. (1987): Synthesis and purification of ^{205}Pb for U-Pb geochronology. *Chem. Geol.* **66**, 110-130.

PARRISH, R.R., HORSTWOOD, M., NOWELL, G., NOBLE, S., TIMMERMANN, H., SHAW, P. & BOWEN, I. (1999). Laser ablation plasma ionization multicollector mass spectrometry: a new method for intracrystal uranium-thorium-lead geochronology using micro-sampling techniques. *In* Ninth Annual V.M. Goldschmidt Conference, p. 219-220. LPI Contribution No. 971, Lunar and Planetary Institute, Houston.

PATCHETT, P.J. & TATSUMOTO, M. (1980a): Hafnium isotope variations in oceanic basalts. *Geophys. Res. Lett.* **7**, 1077-1080.

PATCHETT, P.J. & TATSUMOTO, M. (1980b): A routine high precision method for Lu-Hf isotope geochemistry and chronology. *Contrib. Mineral. Petrol.* **75**, 263-267.

PATCHETT, P.J. & TATSUMOTO, M. (1980c). Lu-Hf total-rock isochron for the eucrite

meteorites. *Nature* **288**, 571-574.

PATCHETT, P.J., KOUVO, O., HEDGE, C.E. & TATSUMOTO, M. (1981). Evolution of continental crust and mantle heterogeneity: evidence from Hf isotopes. *Contrib. Mineral. Petrol.* **78**, 279-297.

ROULEAU, C.M., LOWNDES, D.H., STRAUSS, M.A., CAO, S., PEDRAZA, A.J., GEOHEGAN, D.B., PURETZY, A.A. & ALLARD, L.F. (1996): Effect of ambient gas pressure on pulsed laser ablation plume dynamics and ZnTe film growth. *In* Advanced Laser Processing of Materials - Fundamentals and Applications (R. Singh, D. Norton, L. Laude, J. Narayan & J. Cheung, eds.). Materials Research Society Symposium Proceedings **397**, 119-124.

RUSSELL, W.A., PAPANASTASSIOU, D.A. & TOMBRELLO, T.A. (1978): Ca isotope fractionation on the Earth and other solar system materials. *Geochim. Cosmochim. Acta* **42**, 1075-1090.

SCHERER, E.E., CAMERON, K.L. & BLICHERT-TOFT, J. (2000). Lu-Hf garnet geochronology: Closure temperature relative to the Sm-Nd system and the effects of trace mineral inclusions. *Geochim. Cosmochim. Acta* **64**, 3413-3432.

SCOTT, D.J. & GAUTHIER, G. (1996): Comparison of TIMS (U-Pb) and laser ablation microprobe ICP-MS (Pb) techniques for age determination of detrital zircons from Paleoproterozoic metasedimentary rocks from northeastern Laurentia, Canada, with tectonic implications. *Chem. Geol.* **131**, 127-142.

SILVER, L.T. & DEUTSCH, S. (1963): Uranium-lead isotopic variations in zircon: a case study. *J. Geol.* **71**, 721-758.

STERN, R.A. (1997): The GSC Sensitive High Resolution Ion Microprobe (SHRIMP): analytical techniques of zircon U-Th-Pb age determinations and performance evaluation. *In* Radiogenic Age and Isotopic Studies: Report 10. Geol. Surv. Can., Current Research **1997-F**, 1-31.

STERN, R.A. & BERMAN, R.G. (2000): Monazite U-Pb and Th-Pb geochronology by ion microprobe, with an application to *in situ* dating of an Archean metasedimentary rock. *Chem. Geol.* **172**, 113-130.

STEVENSON, R.K. & PATCHETT, P.J. (1990): Implications for the evolution of continental crust from Hf isotope systematics of Archean detrital zircons. *Geochim. Cosmochim. Acta* **64**, 1683-1697.

TATSUMOTO, M., HEDGE, C.E., DOE, B.R. & UNRUG, D.M. (1972): U-Th-Pb and Rb-Sr measurements on some Apollo 14 lunar samples. *Proc. 3rd Lunar Sci. Conf.* **2**, 1531-1555.

TERA, F. & WASSERBURG, G.J. (1972): U-Th-Pb systematics in three Apollo 14 basalts and the problem of initial Pb in lunar rocks. *Earth Planet. Sci. Letters* **14**, 281-304.

THIRLWALL, M. (2000). Precise Pb isotope analysis of standards and samples using an IsoProbe multicollector ICP-MS: comparisons with doublespike thermal ionization data. *J. Conference Abstracts* **5**, 996.

VERVOORT, J.D. & BLICHERT-TOFT, J. (1999). Evolution of the depleted mantle: Hf isotope evidence from juvenile rocks through time. *Geochim. Cosmochim. Acta* **63**, 533-556.

VERVOORT, J.D., PATCHETT, P.J., GEHRELS, G.E. & NUTMAN, A.P. (1996). Constraints on early Earth differentiation from hafnium and neodymium isotopes. *Nature* **379**, 624-627.

WALDER, A.J. (1997). Advanced isotope ratio mass spectrometry II: isotope ratio measurement by multi collector inductively coupled plasma mass spectrometry. *In* Modern Isotope Ratio Mass Spectrometry (Platzner, I.T., ed.), John Wiley and Sons, Chichester, 83-108.

WETHERILL, G.W. (1956): Discordant uranium-lead ages. *Trans. Amer. Geophys. Union* **37**, 320-326.

WIEDENBECK, M., ALLÉ , P., CORFU, F., GRIFFIN, W.L., MEIER, M., OBERLI, F., VON

QUADT, A., RODDICK, J.C. & SPIEGEL, W. (1995): Three natural zircon standards for U-Th-Pb, Lu-Hf, trace element and REE analyses. *Geostandards Newsletter* **19**, 1-23.

WILLIAMS, I.S. (1998): U-Th-Pb geochronology by ion microprobe. *In* Applications of Microanalytical Techniques to understanding Mineralizing Processes (M.A. McKibben, W.C.P. Shanks III & W.I. Ridley, eds.). Soc. Econ. Geol. Short Course Vol. **7**, 126-142.